Detailed investigation of the low energy secondary electron yield of technical Cu and its relevance for the LHC

R. Cimino,[1,2,*] L. A. Gonzalez,[1,3] R. Larciprete,[1,4] A. Di Gaspare,[1] G. Iadarola,[2] and G. Rumolo[2]

[1]*LNF-INFN, Via E. Fermi 40, 00044 Frascati (Roma) Italy*
[2]*CERN, CH-1211 Geneva 23, Switzerland*
[3]*'Autonoma' University of Madrid, 28049 Madrid, Spain*
[4]*CNR-ISC Istituto dei Sistemi Complessi Via Fosso del Cavaliere 100, 00133 Roma, Italy*

The detailed study of the low energy secondary electron yield (LE-SEY) of technical Cu for low electron energies (from 0 to 20 eV) is very important for electron cloud build up in high intensity accelerators and in many other fields of research. Different devices base their functionalities on the number of electrons produced by a surface when hit by other electrons, namely its SEY, and, in most cases, on its very low energy behavior. However, LE-SEY has been rarely addressed due to the intrinsic experimental complexity to control very low energy electrons. Furthermore, several results published in the past have been recently questioned, allegedly suffering from experimental systematics. Here, we critically review the experimental method used to study LE-SEY and precisely define the energy region in which the experimental data can be considered valid. By analyzing the significantly different behavior of LE-SEY in clean polycrystalline Cu (going toward zero at zero impinging energies) and in its as received technical counterpart (maintaining a significant value in the entire region), we solve most, if not all, of the apparent controversy present in the literature, producing important inputs for better understanding the device performances related to their LE-SEY. Simulations are then performed to address the impact of such results on electron cloud predictions in the LHC.

I. INTRODUCTION

An extremely vast range of research spanning from detectors, photon or electron-multipliers, high power microwave tubes, systems for satellite applications [1], radio-frequency cavities [2], to optics for extreme ultraviolet (EUV) lithography [3], bases some of their essential functionalities on the number of electrons produced by a surface when hit by other electrons. This quantity, called secondary electron yield (SEY), is defined as the ratio of the number of emitted electrons (also called secondary electrons) to the number of incident electrons (also called primary electrons) [4], and is commonly denoted by δ. Its value, its time stability and its dependence on primary electron dose and energy are indeed a crucial issue and an essential ingredient in the design of many devices.

In particular, for particle accelerators with intense and positively charged beams and/or vacuum chambers of small transverse dimensions, electrons can be produced either by the synchrotron radiation hitting the accelerator walls [5,6] or by direct ionization of residual gases. Once the primary electrons are produced, they are accelerated by the electric field of the bunch in the direction perpendicular to the beam direction, creating secondary electrons at the accelerator walls. If the bunch charge and the bunch spacing satisfy certain conditions, a resonance phenomenon called multipacting can be established. When the effective SEY at the chamber walls is larger than unity, the electron population grows rapidly in time with successive bunch passages. This can lead to a high electron density, and, hence, to detrimental effects such as a rapid pressure rise in the vacuum chamber resulting in beam loss. This phenomenon is called electron cloud (EC) build-up, and has been identified as source of limitations of accelerator performances in the SPS, Large Hadron Collider (LHC), the positron rings at the B (Beauty) factories PEP-II, KEKB, etc. [7]. It is now clear that the best performance of present and future accelerators can be achieved if Electron Cloud Effects (ECE) are understood, predicted and finally mitigated. The only way to control and overcome such effects is to ensure a low SEY. At LHC SEY reduction is expected to occur during initial operations (scrubbing or conditioning) and is considered necessary to reach nominal operation [7–10].

Here we would like to address the detailed behavior of SEY at very low impinging electron energy ($E_p < 20$ eV). This low energy part of the SEY spectrum, which we will here call LE-SEY, plays a major role in determining the

performances of many scientific systems and devices but its detailed structure is still under debate. This is even more true for electron cloud oriented accelerator where most of the electrons present in the e-cloud are of very low energy in nature, and have been shown to have peculiar properties in terms of scrubbing [7,8,11–14]. In recent years, detailed studies [5,15–17] on SEY from Cu technical surfaces presented new observations reporting, for the first time, the tendency of SEY not only to reach 1 as E_p approaches 0 eV, but also to stay significantly above 0 for a quite extended energy region, having a minimum SEY of about 0.5–0.7 at E_p as high as 10–20 eV. This low energy behavior was clearly stated to be relative to the actual technical Cu surface studied and a strong warning was given against the extrapolation of such results as being a general property of SEY. More recently, Kaganovich and others [18], put this observation into question suggesting instead that the measured SEY is somehow due to experimental artifacts, since the SEY value at zero impinging energy is and must be zero or close to zero and the SEY curve should nearly monotonically decrease to this value. The authors corroborate such statement with experimental findings taken from the literature [19–24]. Also, some theoretical computations predict a very low SEY at E_p around zero and show a very good agreement between simulated SEY and experimental data [19] for the case of clean Al. In those simulations, the effect of the surface-barrier potential which causes the reflection of incident electrons was also taken into account. The electron reflectivity R_{el} remains low even at 1 eV ($R_{\mathrm{el}} \approx 0.04$), in perfect agreement with experimental results published a few decades ago by Heil and Hollweg [23].

On the other hand, a recent work by Jacques Cazaux [25], while discussing, with a different approach, some theoretical and instrumental issues concerning electrons impinging on a solid surface with $E_p < 10$ eV, performed simulations which are consistent with an increasing R_{el} (up to $R_{\mathrm{el}} = 1$ for $E_p \approx 0$ eV) and with a significantly nonzero SEY for E_p below 10–20 eV. Such simulations are consistent with the data presented and discussed in [5,15,16] and support not only that electron reflectivity R_{el} at zero impact electron energy can be close to 1 but also that SEY value at low impinging energies (from zero to some tens of eV) may have values significantly higher than zero.

On the experimental side, it is clear that the measurements at very low energies are very difficult since it is an intrinsically difficult region to be investigated [26–28], and that, especially at E_p very close to zero, space charge, electromagnetic fields, beam energy resolution, etc. may act on the very low energy electron beam potentially affecting any detailed experimental SEY determination. Still, most of the various systems used for SEY experiments are indeed capable to reproduce the low energy behavior reported [18–24,27] for clean metals, while on technical surfaces, like the LHC Cu used in [5,15,16], such behavior is never reproduced, and a significant SEY is measured. M. Belhaj and coworkers [26], observed that SEY is and stays higher than 0.6 for energies as low as 3 eV for a series of different surfaces exposed to atmosphere. Even if their spectra start at 3 eV, confirming the inherent difficulties to confidently measure SEY at even lower E_p, those data corroborate the observation presented in [5,15,16], and confirm the suggested importance of surface contamination in determining the SEY behavior at very low impinging energy. Such ongoing debate pushed us to quantitatively estimate the confidence with which we can confidently measure the LE-SEY in general, and more specifically analyze the LE-SEY of LHC Cu technical surface to investigate its effects on e^- cloud simulation.

II. EXPERIMENTAL

Experimentally, dealing with very low electron energies is intrinsically difficult since space charge, spurious residual electromagnetic fields, beam energy resolution, etc. may act on the very low energy electron beam potentially affecting any detailed experimental SEY determination [27,28]. In the design of the setups used to perform such experiments and presently in operation at the Material Science INFN-LNF laboratory of Frascati (Roma), great care has been taken to eliminate spurious effects affecting the determination of LE-SEY. The experimental setup, described in details elsewhere [5,7,8,14–17,29], can operate in UHV (background pressure below 10^{-10} mbar). The use of a μ-metal chamber reduces to less than 5 mG the residual magnetic field at the sample position. Various sample preparation (Ar sputtering, evaporators, fast entry lock, etc.) and sample spectroscopic characterization techniques (LEED-Auger, XPS, UPS, SEY) are then available in "situ".

A. Energy reference

We first need to clarify the energy scale and reference, since this is essential to understand the measured data. The energetics of our system is schematically described in Fig. 1. As clearly discussed in [25,30], in such spectroscopic experiments the energy of the different metals and systems (detectors, samples, guns etc.) align at the Fermi level, while the kinetic energy of any emitted electron is referenced to the vacuum level of the material from which it has been emitted, being the work function W the distance between the Fermi level and the vacuum level for each sample. Any applied voltage, to the gun lenses or to the sample, will then accelerate (or retard) the e^- beam. This is to say that electrons emitted by the gun will reference their kinetic energy to the cathode work function, W_G plus additional, when present, applied gun lens voltages, while electrons interacting with the sample will reference their energy to the sample work function (W_s) for metals, or

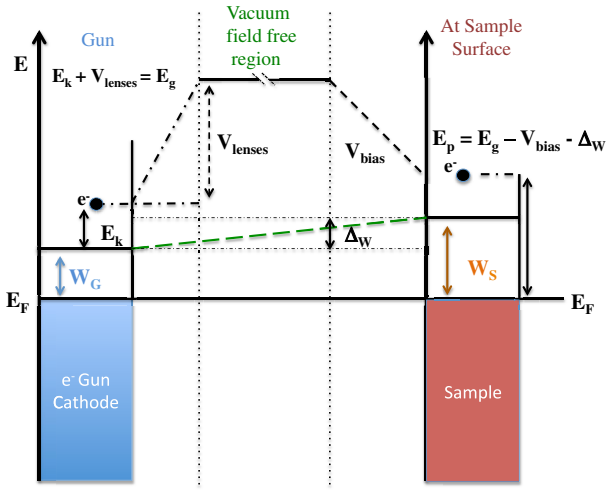

FIG. 1. Schematic of the energetics of our experimental setup. The energy levels are aligned to the equilibrium Fermi level E_F. The symbols used are: W_G is the e- gun cathode work function; W_s is the sample work function (for metals) or $\chi_s + E_{\mathrm{GAP}}$ (for semiconductors and insulators, cases not shown here); Δ W is the difference between W_G and W_s (or $\chi_s + E_{\mathrm{GAP}}$); E_k is the kinetic energy of the e^- just emitted from the cathode; V_{lenses} are the voltage potentials accelerating electrons emitted from the cathode; E_G is the energy of the e^- emitted by the gun into vacuum; V_{bias} is the retarding voltage applied to the sample; E_p is the landing energy (above E_F) of the electrons at the surface, as defined in the text.

electron affinity (χ_s) plus their energy gap (E_{GAP}), for semiconductors and insulators [25,30] and obviously additional, when present, applied bias voltages. For simplicity, we will indicate in the following W_s, keeping in mind that, in case of semiconductors and insulators this quantity should be substituted by $\chi_s + E_{\mathrm{GAP}}$.

In our setup, in order to measure low-energy impinging primary electrons, a negative bias voltage $V_{\mathrm{bias}} \sim -75$ eV, was applied to the sample. Such bias allows us to eliminate space charge problems on the sample, and, more importantly, allows us to work with landing energies close to zero still using the e- gun in an energy region where it is stable ($E_G > V_{\mathrm{bias}} \sim 75$ eV) and focused onto a transverse cross-sectional area of known diameter (here chosen to be either 1.5 mm or 0.5 mm). The landing energy E_p is the energy of the electrons emitted by the gun (E_G) minus the negative applied sample bias voltage (V_{bias}) plus the difference between the e- gun cathode and sample work (or electron affinity + energy gap) functions ($\Delta W = W_s - W_G$). So that:

$$E_p = E_G - V_{\mathrm{bias}} - W_G + W_s = E_G - V_{\mathrm{bias}} + \Delta W. \quad (1)$$

Here we refer all electron energies to the Fermi energy level E_F, which is the common and sample-independent reference for the entire system (see Fig. 1). With this energy reference, the minimum energy of a primary electron interacting and producing a measurable sample current (I_s), with a clean polycrystalline Cu will be the work function (W_{Cu}) of such sample, which is known from literature to be 4.65 eV [31]. Scaling this spectrum (as well as all the others) in this way, eliminates systematic errors linked to the absolute estimate of V_{bias}, E_G, and W_G.

In other words, we set: E_p (above E_F) $= W_s = 4.65$ eV when $E_G - V_{\mathrm{bias}} - W_G = 0$. This implies that, in all spectra, the measured E_p corresponding to the onset of electrons interacting with the solid, (that is when: $E_G - V_{\mathrm{bias}} - W_G \sim W_s$) is an accurate measure of the surface work function W_s (for metals) and $\chi_s + E_{\mathrm{GAP}}$ (for semiconductors and insulators) of the new sample under analysis with respect to W_{Cu}. For completeness, we mention here that in [5,7,8,14–17,29], as well as in most literature on SEY, as reported in [7], the energy scale of the landing electrons was referenced to be zero at $E_p = W_s$ or $\chi_s + E_{\mathrm{GAP}}$ without considering their variation for all samples and sample preparations. This would not significantly alter the conclusions of those papers, since it introduced only a small energy offset between different experiments. In conclusion, this analysis suggests that LE-SEY can be successfully used to measure work functions and its variations upon surface treatment and condition if no experimental artifacts affects the measuring setup.

B. Measuring SEY

The SEY [$\delta(E)$], is defined as the ratio of the number of electrons leaving the sample surface, $I_{\mathrm{out}}(E)$, to the number of incident electrons, $I_p(E)$, per unit area. $I_{\mathrm{out}}(E)$ is the number of electrons emitted from the surface but also the balance between the current flowing from the sample $I_s(E)$ minus the current impinging on the sample, $I_p(E)$, so that:

$$\delta(E) = I_{\mathrm{out}}(E)/I_p(E) \quad (2)$$

and

$$I_{\mathrm{out}}(E) = I_p(E) - I_s(E) \quad (3)$$

thus:

$$\delta(E) = 1 - I_s(E)/I_p(E). \quad (4)$$

The e^- gun emits electrons by thermionic emission and the beam emitted has then an energy broadening related to temperature at which the gun emitter works. In the laboratory we used two different e- guns: one ELG-2, from Kimball Physics, which uses a standard Ta disc cathode and one SL1000, from Omicron, which uses a LaB_6 electron source. The expected width of the primary energy distribution at typical gun working current should be slightly different, since the Ta disk normally requires higher temperature than the LaB_6 to produce the needed e^- flux. The data here presented have been taken using the e^- gun

from Kimball Physics, i.e., with an expected slightly broader width but similar and consistent results are obtained with both sources. In general terms such thermal broadening, indicated by the beam Full Width Half Maximum (FWHM_g), can be assumed to be Gaussian in shape and is known to be ~0.6–1.0 eV, depending on the actual operating gun current and emitter type. Such FWHM_g will than enter in the energetics discussed above, introducing a Gaussian broadening to E_p. Actually, before extrapolating any conclusion from our data, we should indeed experimentally crosscheck that the experimental procedure used (biasing the sample forces us to work in a non-completely field free region) will not affect such FWHM_g value. There are two conceptually identical ways of scanning E_p in the desired energy range, that are obvious from Fig. 1: one implies working with a fixed E_G and vary V_{bias} applied to the sample; the other necessitates to work with a fixed V_{bias} applied to the sample and to vary E_G. It is usually preferred to measure SEY at very low doses (i.e., I_p and $I_s \leq$ a few nA) to avoid surface modification by e^- bombardment (scrubbing) [7,8]. Then a variable sample bias has to be avoided since its use not only would affect significantly the electrostatic fields in the system, especially at high E_p, but would also cause significant leakage currents at increasing V_{bias} especially when trying to work at the lowest possible I_p. The use of a battery box to apply a fixed V_{bias} between 30 and 80 Volts, is then preferred and has shown its advantages eliminating such spurious effects and leak currents. The transverse cross-sectional area can be precisely determined by analyzing the current profile obtained by perpendicularly moving the Faraday cup in front of the gun, as discussed in Ref. [7], and varied between around 0.25 mm^2 for to 3 mm^2 for all energies. The possibility of performing energy scans is offered by most of the e^- guns on the market so that the choice of a fixed V_{bias} and a variable E_G is an experimentally preferable solution which minimizes any potentially detrimental systematic error.

In our setup the SEY measurements are then performed by two subsequent operations: (i) collect the e-gun emitted current $I_p(E_g)$ by using an "ad hoc" designed Faraday cup described elsewhere [7]; (ii) collect the sample electron current $I_s(E)$ as a function of E_p. The SEY value can be considered valid within 5%, taking into account the experimental uncertainties and the intrinsic differences among nominally identical samples. To finally calculate $\delta(E)$ one needs to scale the energy E_G at which $I_p(E)$ is emitted by the e^- gun and measured with the Faraday cup, to the final landing energy E_p by considering the applied retarding voltage V_{bias} and ΔW. The stability of $\delta(E)$ is guaranteed if a series of repeated measurements with the Faraday cup gives very similar $I_p(E)$: a few percent error bars are intrinsic to most of the SEY data and that are due to experimental uncertainties as well as to intrinsic differences from local chemical or morphological sample inhomogeneity.

All SEY curves as a function of E_p are characterized by a maximum value (δ_{max}) reached in correspondence of a certain energy E_{max}. The δ_{max} values and SEY spectra have been extensively studied in recent years [7] and are not the topic of the present paper. Here we would like to validate the capability of our setup to correctly measure LE-SEY, and to benchmark with it the experimental data reported in some of those references.

C. Measuring LE-SEY

In Fig. 2, we pictorially analyze the intrinsic difficulties in dealing with low energy landing energies E_p, especially when they are comparable with FWHM_g. Obviously, for energies $E_G \leq V_{\mathrm{bias}} - \Delta W - \mathrm{FWHM}_g/2$, (see top panel in Fig. 2), even if the Faraday system will correctly measure a nonzero current $I_p(E)$, all electrons impinging on the surface will be electrostatically repelled (reflected) by the higher negative bias voltage, resulting in an I_s ~0, and, consequently, a value of $\delta(E) = 1$ will be obtained. This assumption is not longer valid in absence of any V_{bias} and for all ΔW values, since, obviously, $E_p \leq 0$ is unphysical. With this reasoning in mind, we plot all our measured SEY starting from 1 at $E_G \leq V_{\mathrm{bias}} - \Delta W - \mathrm{FWHM}_g/2$. When all the electrons reach the surface without being repelled by the bias, ($E_G \geq V_{\mathrm{bias}} - \Delta W + \mathrm{FWHM}_g/2$) then they will interact with the surface, and $\delta(E)$ is measured correctly (see bottom panel in Fig. 2). Due to the finite energy width FWHM_g of the e^- gun beam when $V_{\mathrm{bias}} - \Delta W - \mathrm{FWHM}_g/2 \leq E_G \leq V_{\mathrm{bias}} - \Delta W + \mathrm{FWHM}_g/2$ only some of the electrons reach the surface (having an energy$\geq V_{\mathrm{bias}} - \Delta W$), while some other (having an

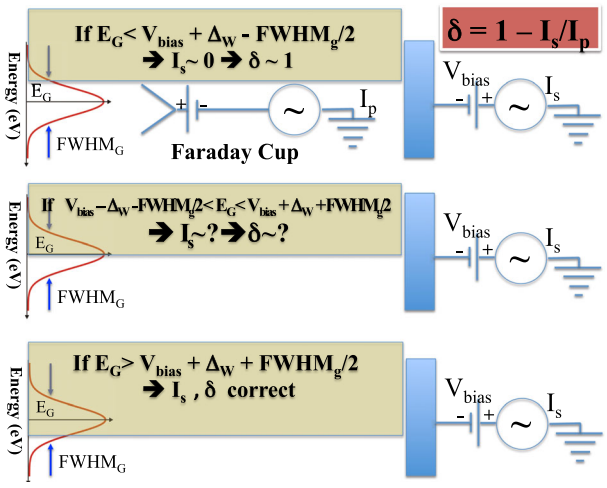

FIG. 2. Schematic of the experimental setup at E_G close to V_{bias} to analyze potential artifacts of the measuring method. In the figure we assume that the e^- beam is Gaussian in nature with a certain FWHM_g.

energy $\leq V_{\text{bias}} - \Delta W$) are repelled by the sample bias. It follows that the measured $\delta(E)$ is inaccurate, since the $I_p(E)$ used in Eq. (4) measures the total number of the e^- emitted by the gun, while $I_s(E)$ refers to those e^- reaching the surface with energy $E_G \geq V_{\text{bias}} - \Delta W$, which will be only a percentage of the ones emitted and measured by the Faraday cup. Their actual number does strongly depend on the energy distribution of the emitted beam. In conclusion, the LE-SEY we measure should consist of three regions: (i) at low energy ($E_G \ll V_{\text{bias}} - \Delta W$), when all impinging electrons are repelled by the biased sample, $\delta(E) = 1$; (ii) at high energy ($E_G \gg V_{\text{bias}} - \Delta W$), when all impinging electrons interact with the sample, $\delta(E)$ is measured correctly; (iii) at ($E_G \sim V_{\text{bias}} - \Delta W$, that is $E_p \sim 0$), when some of the impinging electrons are reflected and some interact with the sample, $\delta(E)$ cannot be accurately measured. The width of this region will measure the e^- gun line width if no other experimental artifacts are affecting our experimental setup.

III. EXPERIMENTAL RESULTS

In this section we present the experimental results that allow us to confidently validate our experimental technique and compare the different literature results. To address such issue we compared different as received Cu technical surfaces before and after having been cleaned by ion sputtering, as checked by XPS analysis. We mention that the geometry and all other experimental conditions were kept constant during the acquisition of the different set of data. The analysis of clean Cu will help us validate the technique and then confidently discuss the LE-SEY of technical Cu either of relevance for ECE studies for the LHC, or for other applications.

A. Clean Cu polycrystalline samples

The SEY measured on an Oxygen-free high thermal conductivity (OFHC) polycrystalline Cu sample cleaned by ion sputtering is shown in Fig. 3. The clean surface was obtained after repeated Ar^+ sputtering cycles of 1 h @ 1.5 keV in an Ar pressure of 5×10^{-6} mbar.

Surface cleanliness was determined by the absence of C and O signals in the XPS spectrum. The SEY curve is measured varying E_p between zero and 1000 eV.

The SEY reported in Fig. 3 shows that the clean polycrystalline Cu has a $\delta_{\text{max}} = 1.4$ at around $E_{\text{max}} =$ 640 eV, consistent with literature results [5,7,14]. The curve shape is similar to the one of other clean metals [19–24,27], with SEY values approaching zero when E_p decreases to zero. A magnification of the very low energy region, shown in Fig. 4, is indeed very instructive. As expected from Fig. 2 and from the previous discussion, the LE-SEY starts at 1. Then, very sharply (FWHM$_g$ = 0.85 eV) decreases to less than 0.1 and slowly increases to higher SEY values. As previously discussed, the threshold

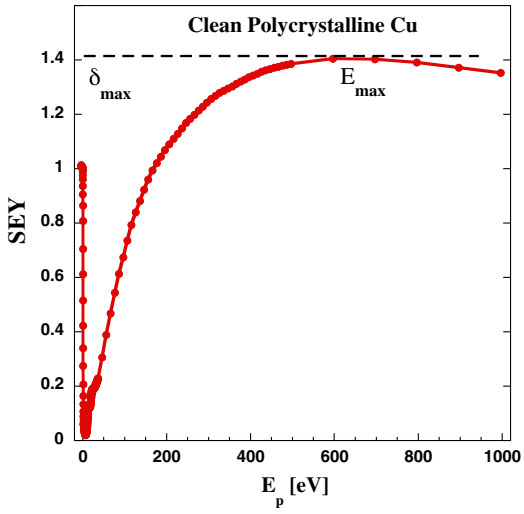

FIG. 3. SEY of a clean polycrystalline Cu as a function of the primary beam energy above E_F.

energy where such decrease takes place has been set at $E_p = W_{\text{Cu}} = 4.65$ eV, being E_F our energy reference. The width of the transition region is measured to have a FWHM = 0.85 eV and is absolutely consistent with the expected thermal broadening deriving from the Ta disk of the Kimball gun. These data suggest that the energy region where our LE-SEY technique is blind, is less than one eV in width. Such "blind region" will be addressed in greater detail in subsequent sections. These data, taken within an unprecedented energy range, spanning over all the low energies of interest, are consistent with previously published data [19–24], on clean samples and with the calculations performed on clean Al [27]. This suggests that clean metals do tend to have LE-SEY values approaching zero at landing electron energies approaching W_S (in

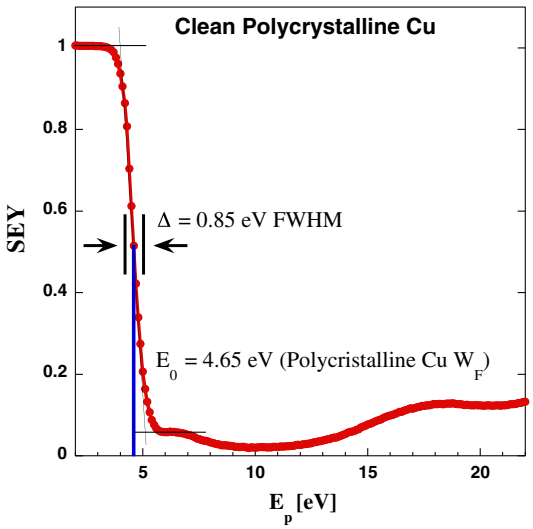

FIG. 4. LE-SEY of a clean polycrystalline Cu as a function of the primary beam energy above E_F.

our energy scale) and to have low LE-SEY values for this entire energy interval. Structures at ∼2 and 14 eV above the W_{Cu} are clearly visible and can be ascribed to plasmon collective excitation occurring in the solid discussed and described elsewhere [27,32].

More importantly, the data confirm the capability of our system to measure with great accuracy LE-SEY values as low as 0.1 at impinging energies less than 1 eV above W_S (or χ_s). In our setup, a quasizero SEY can only be measured if we measure an $I_s(E)$ of the same sign and value of $I_p(E)$. As already discussed, such two quantities are measured independently and the fact that they are of very similar values cannot be ascribed to any experimental artifacts. In case of clean polycrystalline Cu, we can clearly confine in less than 1.0 eV any eventual physical effect bringing the e^- reflectivity to 1 at E_p close to W_S. This is the region where we are blind due to the intrinsic width of our e^- beam.

B. "As received" Cu samples

High resolution LE-SEY curves were measured on several "as received" OFHC Cu samples before cleaning them by ion sputtering. The "as received" samples were rinsed in ethanol and deionized water before being inserted into vacuum. We stress here that the "as received" and the clean Cu were actually the same sample, before and after sputtering, so that the difference in the measured signal cannot be ascribed to any difference in sample positioning or dimensions. Clearly, "as received" is by no means a well-defined chemical state, so that it is expected, and actually measured, that two "as received" Cu samples, of different origin and history, show differences in the measured SEY. As expected, the same surfaces, once clean, were showing nearly identical SEY.

We show in Fig. 5 the SEY of a representative Cu "as received" surface from LHC dipole beam screen [7] and of an OFHC "as received" Cu technical surface and we compare them with the clean polycrystalline Cu. The SEY of the "as received" Cu, while different, in shape, from each other, agrees with literature results, showing a $\delta_{max} \sim 2.0$ at E_{max} ranging from 150 to 350 eV [7]. Ancillary XPS analysis (shown in [8,14] for the LHC Cu) identify a bit more quantitatively such "as received" surfaces without identifying compositional differences to which one can clearly ascribe the difference in SEY. In both surfaces, the Cu signal, which dominates the XPS spectrum of clean Cu, is hardly visible, and the spectrum is dominated by the broad O1s and C 1s core levels, which slightly vary among the two samples and between different measured regions of the same sample. It is outside the scope of the present paper to analyze such differences and understand their origin. Here it is only worth noticing that by "as received" we cannot identify a specific surface composition and this obviously reflects in some differences in the detailed structure and shape of SEY.

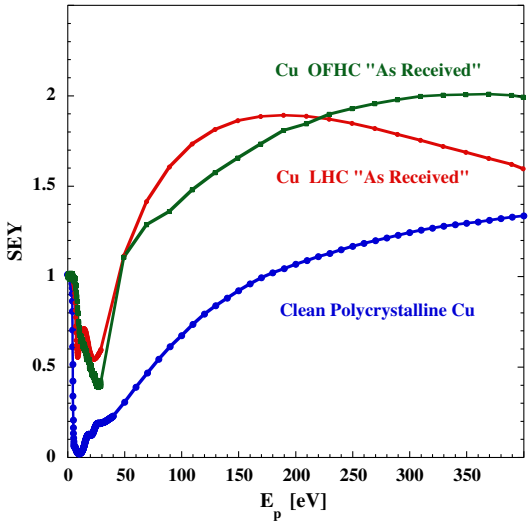

FIG. 5. Experimental SEY curves of an OFHC "as received" Cu; a LHC "as received" Cu and, for comparison, of a clean polycrystalline Cu as a function of E_p above E_F.

In Fig. 6 we zoom into the LE-SEY region between 2 and 27 eV above E_F of the SEY data shown in Fig. 5.

A closer look at Fig. 6 reveals a series of very interesting issues. The differences between clean metal and "as received" surfaces are significant and reproducible. While the LE-SEY of the clean Cu goes and stays close to zero showing no electron reflectivity up to ∼1 eV from W_{Cu}, our data on "as received" Cu surfaces confirm the ability of contaminated surfaces to reflect electrons at very low landing energies and that their δ stay above 0.5–0.7 eV for the entire LE-SEY energy region. We clearly show that we are able to see differences in W_s and $(\chi_s + E_{GAP})$, and

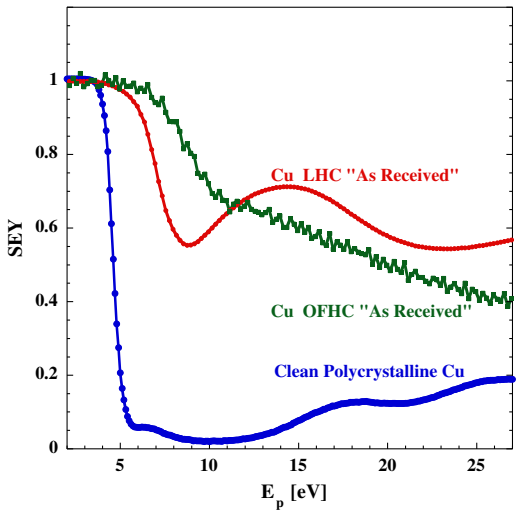

FIG. 6. Experimental LE-SEY curves of an OFHC "as received" Cu; a LHC "as received" Cu and, for comparison, of a clean polycrystalline Cu as a function of E_p above E_F.

to measure their changes as referenced to the clean polycrystalline Cu sample, which sets the energy scale at $W_{\mathrm{Cu}} = 4.65$ eV [31]. Those data show that our technique is clearly able to measure SEY at E_p just above the different samples W_s (or $\chi_s + E_{\mathrm{GAP}}$), with the exception of a "blind region" smaller than 1 eV. Clearly, the as received surfaces exhibit a work function (or $\chi_s + E_{\mathrm{GAP}}$) higher than W_{Cu}, which does not seem to have a very well-defined value. The decrease of the LE-SEY value in the blind region of our apparatus is much reduced. The measured reduction from SEY = 1 to its first flexus is much wider (more than 4 eV) and cannot be ascribed to the experimental FWHM_G broadening. This feature could be ascribed to the presence of nonuniform areas with different work functions (or χ_s and E_{GAP}) even if 4 eV is quite a significant value for such a variation. So, we ascribe this behavior to the enhanced reflectivity R_{el} of the "as received" surface to reflect low landing energy e^-. In fact the data clearly show that, for this as received sample, the reflectivity at landing energy close to W_S (or χ_s) can be assumed to be close to unity, and that the SEY value in the entire LE region is always higher than 0.5 at variance with the clean Cu. This observation clarifies the apparent discrepancy of literature data which can be simply ascribed to the different samples cleanliness, and actual composition and metallicity of the outermost layers, which significantly alter the reflectivity R_{el} at zero landing energies. We show here that SEY and, in particular, its LE part is very surface sensitive and it is strongly affected by the presence of a nonmetallic over layer onto a metal surface. The detailed analysis of why such contaminant layer is so significantly modifying the capability of a surface to reflect low energy impinging e^- is outside the scope of the present work. Space charge or dipole formation in the quasi-insulating over layer, as well as its significant difference in electronic properties from the ones of the clean metal substrates are, indeed, good candidates. Further studies are required to address in detail this issue, especially in the presence of an over-layer with well-defined thickness and composition. Also it may be interesting to confirm that most clean metals show the same low reflectivity behavior observed here for Cu and in [19–24] and to analyze subtle differences that could be related to different metal electronic properties. Surface order and different reconstructions should also have effects on the measured data. Also, the SEY and LE-SEY evolution versus different gas adsorbates can give insight on the different electronic properties of chemically modified surfaces. For technical surfaces, which are of interest here, we confirm the validity of the data presented in [5,7,8,15] and again suggest that detailed studies must be performed to analyze the LE-SEY behavior of any technical surface of interest in the specific device under study. For the case of the Cu sample representative of LHC, we also found a SEY always higher the ~0.5 for the entire LE range, and this is of stimulus to address the effects of such LE-SEY behavior on e^- cloud simulations for the LHC, as it will be done in the final section.

C. Over the "blind region"

Before discussing the potential consequences of the presented results on ECE simulation for the case of the LHC we first shortly analyze the blind region at landing energy close to W_S. As said, in this energy region the finite width of the e^- beam prevents us from measuring the actual number of electrons impinging on the sample. As discussed in Fig. 2 (central panel), in this energy region, the I_p measured by the Faraday cup does not provide the correct number of e^- reaching the surface with energy E_p (above E_F) $\geq W_S$ (which will be called in the following I_p^*).

We can analyze the data in light of this discrepancy, and calculate the actual primary current I_{p^*} by convolving the measured I_p (which is nearly flat and negative in the small LE region of interest) with the impinging e^- beam assumed to have a Gaussian profile with $\mathrm{FWHM}_G = 0.85$ eV. Such analysis is presented in Fig. 7, where we compare the measured I_p with I_p^*. As expected, I_p^* is zero when all electrons are repelled (as in Fig. 2 top panel); is negative and equal to I_p when all e^- interact with the surface (as in Fig. 2, bottom panel); and, in the intermediate region (as in Fig. 2 central panel), is the convolution of a Gaussian with a step function, being exactly 1/2 of I_p at $E_p = W_S$.

In Fig. 8 we compare the measured SEY with that one calculated by using, in Eq. (4), I_p^*. Some peculiarities have to be clarified to better understand the analysis of such corrected SEY. The first regards the region where I_p^* is zero. In this region, as from Eqs. (3) and (4), the SEY is not a defined quantity and has not been plotted. The other aspect

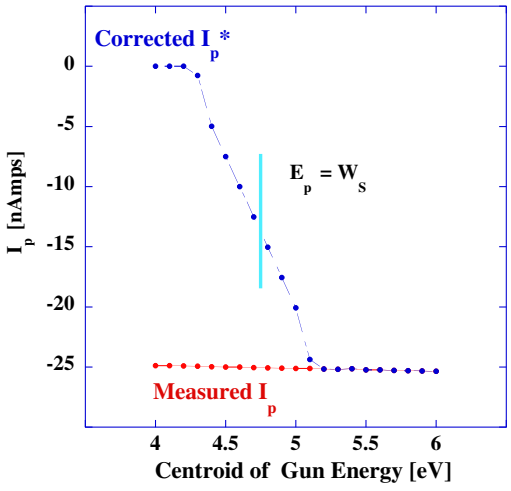

FIG. 7. Comparison between the measured I_p (red dots) and the one obtained by using the corrected I_p^* (blue dots) obtained by convoluting I_p with the Gaussian profile of the e^--beam of $\mathrm{FWHM}_g = 0.85$ eV.

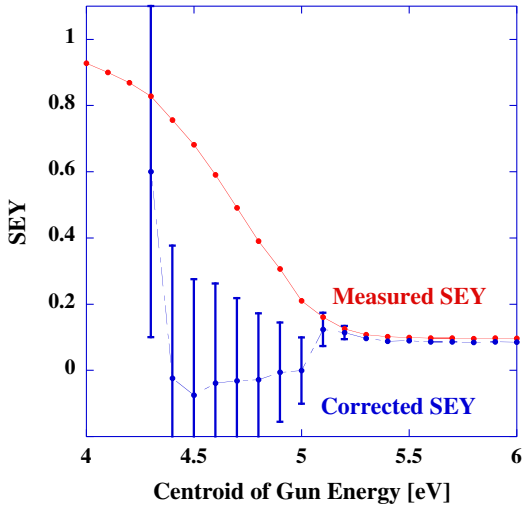

FIG. 8. Comparison between SEY data as obtained dividing the measured I_s by the measured I_p (red dots) and the SEY measured dividing the measured I_s by the corrected I_p^* (blue dots). The corrected I_p^* is obtained by convoluting I_p with a Gaussian profile of the e^--beam of FWHM$_g = 0.85$ eV.

regards the energy scale of the horizontal axis of both Fig. 7 and 8. Such horizontal scale represents the centroid of the Gaussian beam of width FWHM$_g = 0.85$ eV. This does not imply that we have SEY ∼zero at impinging energy less than W_S but that, when the centroid of the Gaussian e^- beam is below W_S there will still be some e^- of energy above W_S that will interact with the surface generating the measured I_s. Finally, the error bars on the corrected SEY have been estimated as due to the decreasing I_p^* current value (down to a few pA). With this in mind, we see that we may extract significant information also from the so-called blind region. Just by assuming a given FWHM$_g$ the corrected I_p^* is, within the error bar, very close to the measured I_s, hence the SEY is close to zero also in the blind region suggesting that no e^- reflectivity rise is occurring for clean Cu even at energy less than 1 eV from W_S. A similar analysis on the different "as received" surfaces, here not shown, confirms, on the other hand, the significant e^- reflectivity measured for such technical samples in the LE-SEY energy region. With this we show that the blind region can still be studied and reduced by analyzing the measured data in light of the finite width of the e^- beam and confirm the same trend as discussed for the entire LE-SEY region, also in the region not directly accessible.

IV. SIMULATIONS

In order to get some hints on what may be the impact of the measured LE-SEY on the e^- cloud buildup [7] for the LHC, PyECLOUD simulations [10,33,34] have been performed for the LHC dipole magnet for the nominal beam at injection energy and chamber parameters as reported in Table I (see details in [34]). Before deciding to introduce in

TABLE I. LHC beam and chamber parameters used in the simulations.

Parameter	Units	
Bunch spacings	ns	25
Beam particle energy	GeV	450
Bunch length (r.m.s.)	m	0.12
Transverse normalised emittances ($\epsilon_x = \epsilon_y$)	μm	3.5
Number of bunches	···	2808
No. of particles per bunch N_b	10^{11}	1.15
Bending field B	T	0.54
Vacuum screen half height	mm	18
Vacuum screen half width	mm	22

the simulation code a more refined and realistic parametrization of the actual experimental LE-SEY curve (which would be the ultimate solution taking care of all the experimental details of the SEY curve, including its LE part) our goal is to see whether small changes in the 0–20 eV SEY region could produce significant differences in simulated e-cloud effects.

The model for the SEY for perpendicular electron incidence as a function of primary energy $\delta(E)$ used for the calculations is based on a parametrization of $\delta(E)$ derived from extensive laboratory measurements, which were carried out on the copper surface of the LHC beam chambers at CERN and in other research institutes [7,12,15,17,35]. In the adopted model we decompose $\delta(E)$ curve in two main components, as shown in Fig. 9:

$$\delta(E) = \delta_{\text{elas}}(E) + \delta_{\text{true}}(E) \tag{5}$$

where $\delta_{\text{elas}}(E)$ and $\delta_{\text{true}}(E)$ correspond respectively to electrons which are elastically reflected by the surface and to the so-called "true secondaries." In this paper and in

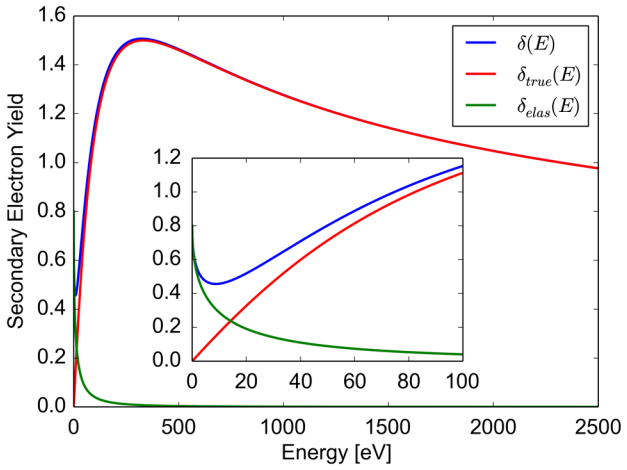

FIG. 9. SEY curve [$\delta(E)$] for $\delta_{\max} = 1.5$ (blue curve), its elastic component $\delta_{\text{elas}}(E)$ (green curve) and its "true secondary" component $\delta_{\text{true}}(E)$. Inset: zoom on the low energy region.

these calculations we sum up in $\delta_{\text{true}}(E)$ also all primary backscattered electrons, which are known to contribute to the total SEY curve [15,36]. This is done not only to simplify the parametrization, but mainly because, in the LE-SEY interval we are dealing with, the separation of true secondary electrons and inelastically backscattered electrons in the total SEY signal cannot be addressed [15,36]. The true secondary component is parametrized [37,38] as:

$$\delta_{\text{true}}(x) = \delta^*_{\text{max}} \frac{sx}{s-1+x^s} \tag{6}$$

where $x = E/E^*_{\text{max}}$, with the value $s \approx 1.35$ as obtained from several measured data sets [15,36]. There are only two free parameters, namely the energy at which the true yield is maximum, E^*_{max}, which has been set to ≈332 eV, as found in measurements, and the effective maximum secondary emission yield δ^*_{max}.

The elastically reflected component is normally parametrized [15] as:

$$\delta_{\text{elas}}(E) = R_0 \frac{(\sqrt{E}-\sqrt{E+E_0})^2}{(\sqrt{E}+\sqrt{E+E_0})^2} \tag{7}$$

with two fit parameters E_0 and R_0. In particular, R_0 is the reflectivity at zero impinging energy. In the following R_0 it will be taken to be equal to 0.8.

The expression for δ_{elas} introduces a minimum in the total SEY curve, as it is seen in Fig. 9 and a value of $\delta(0) = R_0$.

In the following we modify the parametric form of the SEY, introducing differently distributed LE parts on otherwise unchanged curves and parameters. This is shown in Fig. 10:

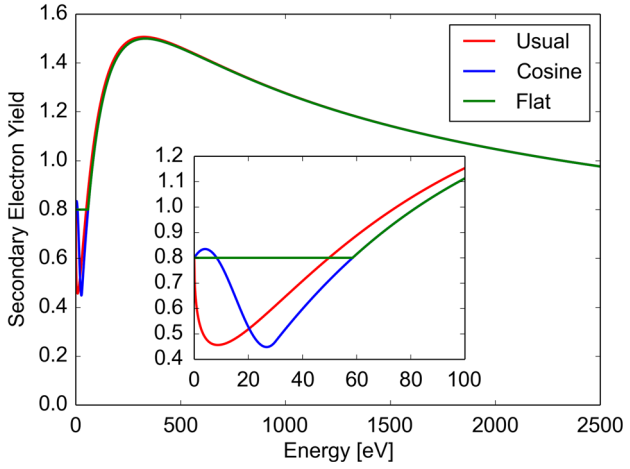

FIG. 10. SEY curve $[\delta(E)]$ for $\delta_{\text{max}} = 1.5$ and $R_0 = 0.8$ for three differently parametrized elastic components $\delta_{\text{elas}}(E)$: Usual parametrization (red curve); Flat parametrization (green curve) and cosine parametrization (blue curve). Inset: zoom on the low energy region.

In one case we assume:

$$\delta_{\text{elas}}(E) = \begin{cases} R_0 - \delta_{\text{true}}(E) & \text{if } \delta_{\text{true}}(E) < R_0, E < E_{\text{max}} \\ 0 & \text{elsewhere} \end{cases} \tag{8}$$

This distribution, called "Flat" in Fig. 10, consists in the simple assumption to have a constant value $\delta(E) = R_0$ for the LE-SEY. Such value was deliberately chosen to be below 1, since, initially, we do not want to study what happened to simulations for $\delta(0) = R_0 = 1$, which is, as previously discussed, in the so-called "blind region" but to see the effect of a significant LE-SEY in the 1 to 20 eV region, where we can confidently measure.

We also study the case in which the elastic component of the SEY is given by:

$$\delta_{\text{elas}}(E) = \begin{cases} R_0 \cos^2\left(\frac{\pi}{2}\frac{E}{E_0}\right) & \text{if } E < E_0 \\ 0 & \text{elsewhere} \end{cases} \tag{9}$$

This distribution, called "Cosine" in Fig. 10, allows having a higher LE-SEY than by using the usual model still maintaining a local minimum in the LE region.

In Fig. 11 we finally show the simulated EC induced heat load as a function of δ_{max} for the three different parametrization of the SEY in the LE region and otherwise identical SEY and simulation parameters. The simulations confirm a significant impact of the LE-SEY on the e^- cloud buildup behavior. In particular the δ_{max} threshold becomes significantly lower for a constant LE-SEY at 0.8 rather than for the usual parametrization, and heat load above threshold gets significantly enhanced. Note that in all three cases the SEY at zero energy has been set to 0.8 suggesting that, more than the actual SEY at 0 eV, it is the overall behavior of the LE-SEY which can significantly influence ECE predictions in LHC. These results call for a more detailed effort to insert in the simulation codes realistic SEY and LE-SEY parametrization to obtain a better simulation accuracy.

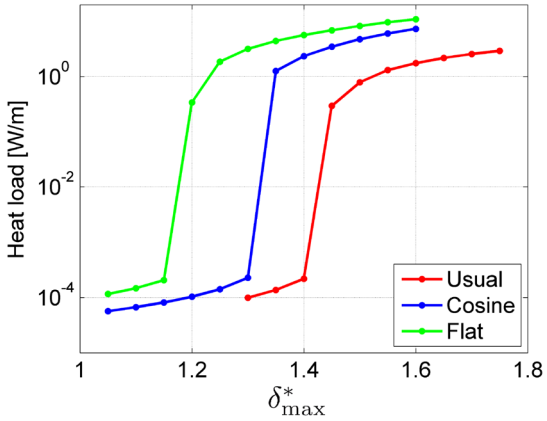

FIG. 11. Simulated heat load as a function of the δ_{max} parameter for the different LE-SEY behaviors.

V. CONCLUSION

We show here that it is possible to measure LE-SEY with great confidence and without experimental artifacts down to 1 eV above sample W_s (in case of metallic surfaces) and EA (in case of semiconductors and insulators) and that the discrepancies recently discussed in literature were mainly due to the different samples studied rather than to any experimental artifact. On the other hand, our preliminary calculations show that the LE-SEY detailed knowledge is indeed important to correctly simulate and predict ECE effects. Therefore a more detailed campaign aimed to measure LE-SEY versus scrubbing and temperature and to feed those results into simulations is mandatory for a detailed analysis of LE-SEY effects on the ECE.

ACKNOWLEDGMENTS

The authors are indebted to A. Romano for initial help. This work was supported by INFN Group V. We acknowledge the staff of DAΦNE-Light for technical assistance.

[1] S. T. Lai, *Fundamentals of Spacecraft Charging: Spacecraft Interactions with Space Plasmas* (Princeton University Press, 2011).
[2] J. R. M. Vaughan, IEEE Trans. Electron Devices **35**, 1172 (1988).
[3] J. Chen, E. Louis, J. Verhoeven, R. Harmsen, C. J. Lee, M. Lubomska, M. van Kampen, W. van Schaik, and F. Bijkerk, Appl. Surf. Sci. **257**, 354 (2010).
[4] H. Seiler, J. Appl. Phys. **54**, R1 (1983).
[5] R. Cimino, Nucl. Instrum. Methods Phys. Res., Sect. A **561**, 272 (2006).
[6] R. Cimino, V. Baglin, and I. R. Collins, Phys. Rev. ST Accel. Beams **2**, 063201 (1999).
[7] R. Cimino and T. Demma, Int. J. Mod. Phys. A **29**, 1430023 (2014).
[8] R. Cimino, M. Commisso, D. Grosso, T. Demma, V. Baglin, R. Flammini, and R. Larciprete, Phys. Rev. Lett. **109**, 064801 (2012).
[9] O. Dominguez, K. Li, E. Metral, G. Rumolo, F. Zimmermann, and H. Maury Cuna, Phys. Rev. ST Accel. Beams **16**, 011003 (2013).
[10] G. Iadarola, G. Arduini, V. Baglin, H. Bartosik, J. Esteban Muller, G. Rumolo, T. L. Shaposhnikova, E. F. Zimmermann, O. Domnguez, and G. H. I. Maury Cuna, in *Proceedings of the 4th International Particle Accelerator Conference, IPAC-2013, Shanghai, China, 2013* (JACoW, Shanghai, China, 2013), p. 1131.
[11] V. Baglin, J. Bojko, O. Gröbner, B. Henrist, N. Hilleret, C. Scheuerlein, and M. Taborelli, CERN LHC-Project-Report-433, 2000.
[12] V. Baglin, I. Collins, B. Henrist, N. Hilleret, and G. Vorlaufer, CERN LHC Project Report 472, 2001.
[13] N. Hilleret, C. Scheuerlein, and M. Taborelli, Appl. Phys. A **76**, 1085 (2003).
[14] R. Larciprete, D. R. Grosso, M. Commisso, R. Flammini, and R. Cimino, Phys. Rev. ST Accel. Beams **16**, 011002 (2013).
[15] R. Cimino, I. R. Collins, M. A. Furman, M. Pivi, F. Ruggiero, G. Rumolo, and F. Zimmermann, Phys. Rev. Lett. **93**, 014801 (2004).
[16] R. Cimino, in *Proceedings of the 31st ICFA Advanced Beam Dynamics Workshop on Electron-Cloud Effects "ECLOUD 04", Napa, CA*, CERN Yellow Report No. CERN-2005-001.
[17] R. Cimino and I. R. Collins, Appl. Surf. Sci. **235**, 231 (2004).
[18] A. N. Andronov, A. S. Smirnov, I. D. Kaganovich, E. A. Startsev, Y. Raitses, and V. I. Demidov, Report No. CERN-2013-002, p. 161.
[19] I. M. Bronshtein and B. S. Fraiman, *Secondary Electron Emission* (Atomizdat, Moscow, Russia, 1969).
[20] G. A. Haas, J. Vac. Sci. Technol. **13**, 479 (1976).
[21] I. M. Bronshtein and V. Roshchin, *Sov. J. Tech.-Phys **3**, 2271 (1958).*
[22] I. H. Khan, J. P. Hobson, and R. Armstrong, Phys. Rev. **129**, 1513 (1963).
[23] H. Heil and J. V. Hollweg, Phys. Rev. **164**, 881 (1967).
[24] Z. Yakubova and N. A. Gorbatyi, *Russ. Phys. J. **13**, 1477 (1970).*
[25] J. Cazaux, J. Appl. Phys. **111**, 064903 (2012).
[26] M. Belhaj, J. Roupie, O. Jbara, J. Puech, N. Balcon, and D. Payan, Report No. CERN-2013-002, p. 137.
[27] J. Roupie, O. Jbara, T. Tondu, M. Belhaj, and J. Puech, J. Phys. D **46**, 125306 (2013).
[28] J. Wang, P. Wang, M. Belhaj, and J.-C. M. Velez, IEEE Trans. Plasma Sci. **40**, 2773 (2012).
[29] D. R. Grosso, M. Commisso, R. Cimino, R. Larciprete, R. Flammini, and R. Wanzenberg, Phys. Rev. ST Accel. Beams **16**, 051003 (2013).
[30] J. Cazaux, J. Appl. Phys. **110**, 024906 (2011).
[31] K. Jakobi, *Work Function Data* (Springer Materials - The Landolt-Börnstein Database, 1993).
[32] A. Dittmar-Wituski, M. Naparty, and J. Skonieczny, J. Phys. C **18**, 2563 (1985).
[33] G. Iadarola and G. Rumolo, Report No. CERN-2013-002, p. 189.
[34] G. Iadarola, Ph.D. thesis, U. Naples (main) (2014), http://cds.cern.ch/record/1705520?ln=en.
[35] B. Henrist, N. Hilleret, M. Jimnez, C. Scheuerlein, M. Taborelli, and G. Vorlaufer, Report No. CERN-2002-001.
[36] M. A. Furman and M. T. F. Pivi, Phys. Rev. ST Accel. Beams **5**, 124404 (2002).
[37] J. R. Young, J. Appl. Phys. **28**, 524 (1957).
[38] A. J. Dekker, *Secondary Electron Emission* (Academic Press, New York, 1958), p. 251.